技術論文

Reduced-order Modeling of Intake Air Dynamics in Single-cylinder Four-stroke Engine

Shun-ichi Akama　Yasunori Murayama　Shigeho Sakoda

当論文は19th Small Engine Technology Conferenceにて発表され、High Quality Paper Awardを得たものです。

Reprinted with permission from SAE Int. J. Engines, December, 2013, 6:2092-2099.
DOI:10.4271/2013-32-9041

要旨

サージタンクのない自然吸気4ストロークガソリンエンジンの吸気ダイナミクスを低次元モデリングする手法を提案する。これにより吸気マニフォールド圧力を組み込みマイコンでリアルタイムに推定することが可能になる。なお、このモデリング手法は単気筒エンジン、および、独立スロットルを備えた多気筒エンジンに適用することができる。本稿ではまず吸気のダイナミクスについて図説し、次いで吸気マニフォールド圧力の推定手法を説明し、最後に本手法の実験結果を紹介する。

Abstract

This study deals with reduced-order modeling of intake air dynamics in single-cylinder four-stroke naturally-aspirated spark-ignited engines without surge tanks. It provides an approximate calculation method for embedded micro computers to estimate intake manifold pressures in real time. The calculation method is also applicable to multi-cylinder engines with individual throttle bodies since the engines can be equated with parallelization of the single-cylinder engines. In this paper, we illustrate the intake air dynamics, describe a method to estimate the intake manifold pressures, and show experimental results of the method.

1 INTRODUCTION

1-1. BACKGROUND

This paper proposes a real-time calculation method for automotive embedded computers to estimate transient responses of intake manifold pressures in motorcycle engines: single-cylinder four-stroke engines or multi-cylinder four-stroke engines equipped with individual throttle bodies (Fig. 1-left). The paper starts from calculation methods to estimate intake manifold pressures of four-wheel automotive engines [1,2,3,4] (Fig. 1-right), and modifies them for motorcycle engines.

The intake manifold pressures are vital to control air-fuel ratios in port-injection gasoline engines; the pressures are strongly associated with masses of intake air sucked into cylinders, and moreover, they determine injection amounts per unit time of injectors. For example, usual electronic control units of four-wheel automotive engines estimate the intake manifold pressures from air mass flows through throttle valves, next they calculate the required fuel amounts from the estimated intake manifold pressures, and finally they compute the injection times from the required fuel amounts. In short, estimating the pressure, the control units compensate differences between the air masses through the throttle valves and the air masses sucked into the cylinders.

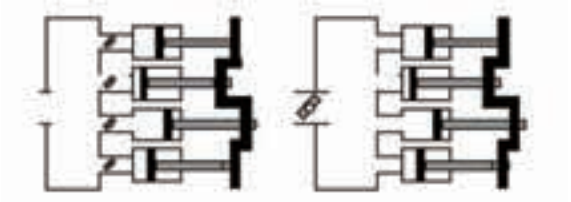

Figure 1: A common motorcycle engine with individual throttle bodies (left) and a common four-wheel automotive engine with a single throttle body (right).

There are three big differences between motorcycle engines and four-wheel automotive engines (Fig. 1). The differences disallow us to estimate the intake manifold pressures in the motorcycle engines by utilizing the estimation methods for the four-wheel automotive engines [1,2,3,4].

- Motorcycle engines are rarely equipped with surge tanks between their throttle valves and intake valves. Hence, their intake manifold volumes are often smaller than their swept volumes. On the other hand, four-wheel automotive engines usually have surge tanks, therefore, their intake manifold volumes are much larger than their swept volumes.
- Each cylinder has its own throttle valve in motorcycle engines. Thus, the air flow through the throttle valve changes during one engine cycle. On the other hand, common four-wheel automotive engines are even-firing single-throttle engines. In such an engine, the air flow through the throttle valve is continuous and smooth since any of its cylinders are in their intake strokes.
- Equivalent moments of inertia about crank shafts of motorcycle engines are much smaller than those of four-wheel automotive engines. Therefore, engine rotational velocities of motorcycle engines increase or decrease much more sharply than those of four-wheel automotive engines. Especially in single-cylinder motorcycle engines, their rotational velocities are perturbed significantly during engine cycles.

The widely-used estimation methods [1,2,3,4,5] assume that the intake air flows are independent from crank angles of the engines. This assumption is validated by the above-mentioned characteristics of the four-wheel automotive engines. However, the intake air flows in the motorcycle engines depend strongly on crank angles; the intake manifold pressures decrease quickly in intake strokes and increase slowly in other strokes. Such pressure changes are caused by the characteristics of the motorcycle engines, and they preclude applications of the estimation methods for the four-wheel automotive engines.

Remark that we can estimate the air flows from the first-principle simulations [6,7]. However, such simulations require too rich computational resource for automotive embedded computers to calculate them in real time. To compute the air flows in real time, it is required to replace the physical principles with statistical approximations.

1-2. KEY POINTS

This paper derives a simple computational model of the intake air dynamics from a view point of enthalpy flows. The followings are the differences from the conventional estimation methods [1,2,3,4] and the first-principle simulations [5,6]. They are key points to simplify the computational model of the intake air dynamics.

1. This paper exploits structures inherent in typical motorcycle engines: small ratios of their intake manifold volumes to their swept volumes, large ratios of opening areas of their intake valves to their combustion chamber volumes, and so on. Due to these structures, the intake manifolds and cylinders reach states of thermodynamic equilibria in negligibly short times.
2. We focus on factors of importance for air-fuel ratio controls: (1) the intake manifold pressures from the intake valve closing (IVC) timings to the intake valve opening (IVO) timings, (2) the intake manifold pressures at the IVC timings, and (3) residual gas densities at the exhaust valve closing (EVC) timings. Factors other than those listed above (e.g. the intake manifold pressures during periods of valve overlaps) are of secondary importance.
3. Periods of valve overlaps are approximated by zeros in the computational model. Instead, amounts of residual gas and shortcut gas are estimated by using look-up tables which are experimentally calibrated.
4. Intake pulsations are calculated independently from the air flows, and they are modeled as damping oscillations with four parameters: interval, damping coefficient, initial amplitude, and initial phase. These parameters are determined from look-up tables which are adjusted experimentally.

5. Changes of engine rotational velocities are predicted from cylinder pressures, inertia torques, back torques, and frictions. The prediction compensates sharp increase or decrease of the engine rotational velocities.

Compared to the estimation methods [1,2,3,4], the proposed method requires richer computational resource to calculate the air flow and the engine rotational velocity. Nevertheless, it keeps feasibility of real-time computing due to the above-mentioned simplifications.

1-3. APPLICATIONS

The proposed method is of service to the following technical areas:

- The method can be utilized as a soft-sensor of the intake manifold pressure. Some of low cost motorcycles with fuel injection systems equip only throttle position sensors, and they equip neither intake manifold pressure sensors nor air flow sensors. Since the intake manifold pressures are vital for the fuel injection controls, the proposed method is useful for such motorcycles.
- Combining the method with a prediction method of a throttle position provides a predictive value of the intake manifold pressure, which is informative for computation of asynchronous injection. Especially for motorcycles with electronic throttle control systems, the predictive value can be accurately calculated by exploiting response lags of the throttle controls.
- The method increases accuracy of backfire detection. Even weak backfires are detectable by comparison of measured intake manifold pressures with estimated intake manifold pressures. In particular, the method is suitable for the backfire detection under unstationary driving conditions since it is applicable to estimation of transient intake manifold pressures.

1-4. ORGANIZATION

Chapter "FLOWS AND STAGNATION" gives a mathematical description of flows and stagnation in the intake manifolds. Chapter "AIR MODEL" illustrates the intake air model. Chapter "CALIBRATION OF AIR MODEL" sketches how to adjust our method. Chapter "EXPERIMENTAL RESULTS" shows our results of experiments. The final chapter concludes the paper.

2 FLOWS AND STAGNATION

This chapter provides mathematical descriptions on flows and stagnation illustrated in Fig. 2. In the figure, the index 2 denotes a throttle valve, and the indices 1 and 3 denote its upstream and downstream, respectively.

2-1. SUBSONIC FLOW

Consider an enthalpy balance along a diabatic subsonic flow from the upstream to the throttle valve:

$$\frac{1}{2}\left(\frac{v_1}{C}\right)^2 + \frac{\kappa}{\kappa - 1}\frac{P_1}{r_1} = \frac{1}{2}\left(\frac{v_2}{C}\right)^2 + \frac{\kappa}{\kappa - 1}\frac{P_2}{r_2}$$

where C is a discharge coefficient, κ is a specific heat ratio, v is a flow velocity, P is a static pressure, and r is a density. In the above equation, the discharge coefficient indicates the enthalpy balance. If the flow is lossless, then the coefficient is equal to the unity.

Next, let S_1 and S_2 denote a cross-sectional area of the upstream and a valve-opening area of the throttle, respectively. From the equation of continuity, we have

$$S_1 r_1 v_1 = S_2 r_2 v_2 .$$

Moreover, modeling the diabatic flow as a polytropic process, we get

$$\frac{P_2}{P_1} = \left(\frac{r_2}{r_1}\right)^n$$

with n denoting the polytropic index. Various thermodynamical processes can be represented by the polytropic process; an isobaric process by $n = 0$, an isothermal process by $n = 1$, an isentropic process by $n = \kappa$, and an isochoric process by $n = \infty$. In case of an adiabatic expansion process, $n = \kappa$ if all of its internal energy is converted to a work, $1 < n < \kappa$ if a

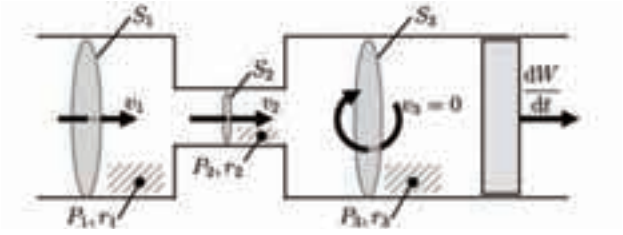

Figure 2: The flows and stagnation in the intake system.

part of its internal energy is converted to a work, and $n = 1$ if none of its internal energy is converted to a work.

2-2. CHOKED FLOW

The flow is caused by propagation of the pressure difference, but the propagation velocity cannot exceed the sonic velocity. Therefore, the mass flow rate becomes saturated, that is "choked", when the flow velocity reaches the propagation velocity.

Let $\gamma = P_2/P_1$. Then, solving the equations in the previous section, we can see that the mass flow rate is saturated when γ satisfies

$$0 = \frac{n-1}{2}\left(\frac{S_2}{S_1}\right)^2 \gamma^{1+\frac{1}{n}} - \frac{n+1}{2}\gamma^{1-\frac{1}{n}} + 1 .$$

Let γ^* denote the solution of the above equation. Then, γ^* corresponds to the critical pressure ratio; if $P_2/P_1 > \gamma^*$, the flow is subsonic, otherwise, it is choked. On the assumption that $S_2/S_1 \simeq 0$, the solution can be approximated by

$$\gamma^* \simeq \left(\frac{2}{n+1}\right)^{\frac{n}{n-1}} .$$

The mass flow rate of the choked flow is equal to that of the saturated subsonic flow. Hence, it is given by solving the following equations:

$$\frac{1}{2}\left(\frac{v_1}{C}\right)^2 + \frac{\kappa}{\kappa-1}\frac{P_1}{r_1} = \frac{1}{2}\left(\frac{v_S}{C}\right)^2 + \frac{\kappa}{\kappa-1}\left(\frac{P_S}{r_S}\right),$$

$$S_1 r_1 v_1 = S_2 r_S v_S ,$$

$$\frac{P_S}{P_1} = \left(\frac{r_S}{r_1}\right)^n,$$

$$P_S = \gamma^* P_1$$

where P_S, r_S, and v_S denote the static pressure, density, and velocity of the saturated subsonic flow, respectively.

2-3. STAGNATION OF SUBSONIC FLOW

When the subsonic flow stagnates in the intake manifold, the enthalpy balance is described by

$$\frac{1}{2}v_2^2 + \frac{\kappa}{\kappa-1}\frac{P_2}{r_2} = \frac{1}{2}v_3^2 + \frac{\kappa}{\kappa-1}\frac{P_3}{r_3} .$$

And, the equation of the continuity is given by

$$\frac{\mathrm{d}}{\mathrm{d}t}(V_3 r_3) = S_3 r_3 v_3 = S_2 r_2 v_2$$

with V_3 being a volume of the stagnation region. Moreover, the energy of the stagnation region changes as

$$\frac{\mathrm{d}}{\mathrm{d}t}\left(\frac{1}{\kappa-1}P_3 V_3\right) + \frac{\mathrm{d}W}{\mathrm{d}t} = \left(\frac{1}{2}v_2^2 + \frac{\kappa}{\kappa-1}\frac{P_2}{r_2}\right) S_2 r_2 v_2 .$$

In the above equation, W denotes a work of the piston (Fig. 2). The above equation means that a change rate of the energy of the stagnation region is equal to the enthalpy of the flow per unit time.

2-4. STAGNATION OF CHOKED FLOW

The equations in the previous section are not true for the choked flow since the pressure P_2 and density r_2 have no relation to the mass flow rate in the choked flow. Instead, from conservation of mass and energy along the choked flow, it follows that.

$$\frac{\mathrm{d}}{\mathrm{d}t}\left(V_3 r_3\right) = S_2 r_S v_S ,$$

$$\frac{\mathrm{d}}{\mathrm{d}t}\left(\frac{1}{\kappa-1}P_3 V_3\right) + \frac{\mathrm{d}W}{\mathrm{d}t} = \left(\frac{1}{2}v_S^2 + \frac{\kappa}{\kappa-1}\frac{P_S}{r_S}\right) S_2 r_S v_S .$$

3 AIR MODEL

This chapter derives a computational model of the intake air flow illustrated in Fig. 3. The model is called "air model," which is composed of the following subsystems (Fig. 4).

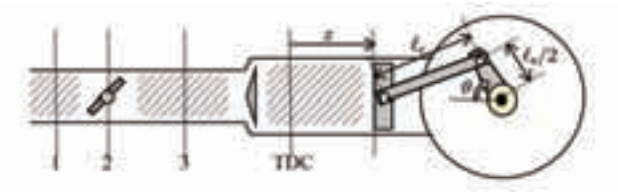

Figure 3: The intake system of a single-cylinder engine.

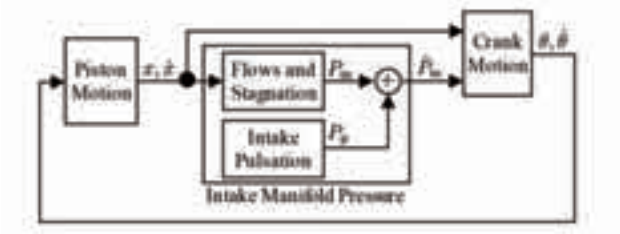

Figure 4: The block diagram of the air model.

3-1. PISTON MOTION

Let x denote the piston position and θ do the crank angle. They are set to zeros at the compression TDC. The positive directions of the x-axis and θ-axis are the same as the direction in which the crank rotates forward. For simplicity, we assume that the crankshaft offset and piston offset are negligibly small. Then, the piston position x and the piston velocity $\dot{x}$ are given by

$$x = \ell_c\left(1-\sqrt{1-\frac{\ell_s^2}{4\ell_c^2}(\sin\theta)^2}\right)+\frac{\ell_s}{2}(1-\cos\theta),$$

$$\frac{dx}{dt}=\frac{d\theta}{dt}\left(\frac{\ell_s^2}{4\ell_c}\frac{\sin\theta\cos\theta}{\sqrt{1-\frac{\ell_s^2}{4\ell_c^2}(\sin\theta)^2}}+\frac{\ell_s}{2}\sin\theta\right)$$

where ℓ_c is the length of the connecting rod and ℓ_s is the length of the stroke.

3-2. INTAKE MANIFOLD PRESSURE

In this section, the indices 1, 2, and 3 indicate the air cleaner, throttle valve, and intake manifold, respectively.

3-2-1. From IVC Timing to IVO Timing

If the flow through the throttle valve is subsonic, we have

$$\frac{1}{2}\left(\frac{v_1}{C}\right)^2+\frac{\kappa}{\kappa-1}\frac{P_1}{r_1}=\frac{1}{2}\left(\frac{v_2}{C}\right)^2+\frac{\kappa}{\kappa-1}\frac{P_2}{r_2},$$

$$S_1r_1v_1 = S_2r_2v_2,$$

$$\frac{P_2}{P_1}=\left(\frac{r_2}{r_1}\right)^n,$$

$$\frac{1}{2}v_2^2+\frac{\kappa}{\kappa-1}\frac{P_2}{r_2}=\frac{1}{2}v_3^2+\frac{\kappa}{\kappa-1}\frac{P_3}{r_3},$$

$$\frac{d}{dt}(V_3r_3) = S_3r_3v_3 = S_2r_2v_2,$$

$$\frac{d}{dt}\left(\frac{1}{\kappa-1}P_3V_3\right)=\left(\frac{1}{2}v_2^2+\frac{\kappa}{\kappa-1}\frac{P_2}{r_2}\right)S_2r_2v_2.$$

From the above six equations, we can calculate v_1, v_2, v_3, P_2, r_2, $\dot{P}_3$, and $\dot{r}_3$, given P_1, r_1, S_1, S_2, S_3, n, κ, and V_3.

If the flow through the throttle valve is choked, then the flow is derived from the following equations:

$$\frac{1}{2}\left(\frac{v_1}{C}\right)^2+\frac{\kappa}{\kappa-1}\frac{P_1}{r_1}=\frac{1}{2}\left(\frac{v_S}{C}\right)^2+\frac{\kappa}{\kappa-1}\frac{P_S}{r_S},$$

$$S_1r_1v_1 = S_2r_Sv_S,$$

$$\frac{P_S}{P_1}=\left(\frac{r_S}{r_1}\right)^n,$$

$$P_S = \gamma^*P_1,$$

$$\frac{d}{dt}(V_3r_3) = S_2r_Sv_S,$$

$$\frac{d}{dt}\left(\frac{1}{\kappa-1}P_3V_3\right)=\left(\frac{1}{2}v_S^2+\frac{\kappa}{\kappa-1}\frac{P_S}{r_S}\right)S_2r_Sv_S$$

where the suffix `s' corresponds to a boundary state between the subsonic flow and choked flow. Solving the above six equations, we obtain v_1, v_S, P_S, r_S, $\dot{P}_3$, and $\dot{r}_3$, given P_1, r_1, S_1, S_2, n, κ, and V_3.

3-2-2. At IVO Timing

For computational simplicity, the air model computes the intake manifold pressure as if the period of the valve overlap were zero, that is, as if the EVC timing were located at the IVO timing. For further simplicity, the air model assumes that the gases in the intake manifold and the cylinder reach a state of thermodynamic equilibrium

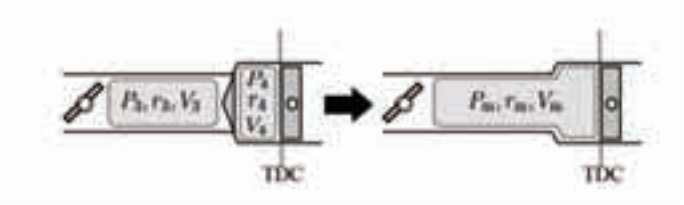

Figure 5: The approximate equilibrium at the IVO timing.

at the IVO timing (Fig. 5). These simplifications reduce the estimation accuracy from the IVO timing to the actual EVC timing. However, by artificially adjusting the cylinder pressure and density just before the IVO timing, the air model can recover the accuracy after the actual EVC timing.

Consider a situation just before the IVO timing. Let P_3, r_3, and V_3 denote the intake manifold pressure, density, and volume, respectively. Similarly, let P_4, r_4, and V_4 denote the cylinder pressure, density, and volume, respectively. If the intake manifold and the cylinder reach a state of thermodynamic equilibrium at the moment of the IVO timing, we have

$$P_{\mathrm{m}} = \frac{P_3V_3 + P_4V_4}{V_3 + V_4},$$

$$r_{\mathrm{m}} = \frac{r_3V_3 + r_4V_4}{V_3 + V_4},$$

$$V_{\mathrm{m}} = V_3 + V_4$$

where the suffix `m' represents a unified region of the intake manifold and the cylinder. The pressure P_4 and density r_4 are calibrated so that the estimation accuracy recovers after the actual EVC timing.

Remark that the above adjustments are validated by characteristic structures of the motorcycle engines:

- Because of a small ratio of the intake manifold to the stroke volume, the residual gas diffused in the intake manifold is scavenged in the intake stroke and it does not remain after the intake stroke.
- Due to a large ratio of the opening area of the intake valve to the combustion chamber volume, the unified region reaches the equilibrium before the EVC timing.

In return for the computational simplicity, the estimation accuracy is reduced during the period of the valve overlap. The estimation accuracy can be improved by computing gas transfers during the period [8,9,10]. However, this paper places the computational simplicity ahead of the estimation accuracy and tolerates the estimation error. This is because the proposed method is designed to the air-fuel ratio control, which is not sensitive to the estimation error during the period.

3-2-3. From IVO Timing to Next IVC Timing

On the assumption that a flow through the intake valve is lossless, this paper treats the intake manifold and the cylinder as a unified region.

Let S_4 be the cross-sectional area of the cylinder and V_{TDC} be the combustion chamber volume. Then, the volume of the unified region is given by

$$V_{\mathrm{m}} = V_3 + V_{\mathrm{TDC}} + S_4x .$$

When the flow is subsonic, it follows that

$$\frac{1}{2}\left(\frac{v_1}{C}\right)^2 + \frac{\kappa}{\kappa - 1}\frac{P_1}{r_1} = \frac{1}{2}\left(\frac{v_2}{C}\right)^2 + \frac{\kappa}{\kappa - 1}\frac{P_2}{r_2},$$

$$S_1r_1v_1 = S_2r_2v_2 ,$$

$$\frac{P_2}{P_1} = \left(\frac{r_2}{r_1}\right)^n ,$$

$$\frac{1}{2}v_2^2 + \frac{\kappa}{\kappa - 1}\frac{P_2}{r_2} = \frac{1}{2}v_{\mathrm{m}}^2 + \frac{\kappa}{\kappa - 1}\frac{P_{\mathrm{m}}}{r_{\mathrm{m}}},$$

$$\frac{\mathrm{d}}{\mathrm{d}t}\left(V_{\mathrm{m}}r_{\mathrm{m}}\right) = S_3r_{\mathrm{m}}v_{\mathrm{m}} = S_2r_2v_2 ,$$

$$\frac{\mathrm{d}}{\mathrm{d}t}\left(\frac{1}{\kappa - 1}P_{\mathrm{m}}V_{\mathrm{m}}\right) + P_{\mathrm{m}}\frac{\mathrm{d}V_{\mathrm{m}}}{\mathrm{d}t} = \left(\frac{1}{2}v_2^2 + \frac{\kappa}{\kappa - 1}\frac{P_2}{r_2}\right)S_2r_2v_2 .$$

And, when the flow is choked, then

$$\frac{1}{2}\left(\frac{v_1}{C}\right)^2 + \frac{\kappa}{\kappa-1}\frac{P_1}{r_1} = \frac{1}{2}\left(\frac{v_S}{C}\right)^2 + \frac{\kappa}{\kappa-1}\frac{P_S}{r_S},$$

$$S_1 r_1 v_1 = S_2 r_S v_S,$$

$$\frac{P_S}{P_1} = \left(\frac{r_S}{r_1}\right)^n,$$

$$P_S = \gamma^* P_1,$$

$$\frac{\mathrm{d}}{\mathrm{d}t}(V_m r_m) = S_2 r_S v_S,$$

$$\frac{\mathrm{d}}{\mathrm{d}t}\left(\frac{1}{\kappa-1}P_m V_m\right) + P_m\frac{\mathrm{d}V_m}{\mathrm{d}t} = \left(\frac{1}{2}v_S^2 + \frac{\kappa}{\kappa-1}\frac{P_S}{r_S}\right)S_2 r_S v_S.$$

3-2-4. Superposition of Intake Pulsation

The intake pulsation occurs by the water hammer effect and air column resonance. It can be modeled as a damping oscillation; its interval is derived from the sonic velocity and a distance from the air cleaner to the intake valve, its amplitude is proportional to the mass flow rate in the last cycle, and its damping time constant depends on a viscosity resistance of the gas. Let t_{IVC} denote the IVC timing, and A_p, τ_p, ω_p, and θ_p denote the initial amplitude, damping time constant, angular velocity, and initial phase angle, respectively. Then, we have

$$P_p = A_p e^{-(t-t_{IVC})/\tau_p}\sin\left(\omega_p(t-t_{IVC}) + \theta_p\right).$$

The air model computes the above equation separately from the intake air flow described in the previous sections, and superposes it to the intake manifold pressure, that is,

$$\hat{P}_3 = P_3 + P_p$$

from the IVC timing to the IVO timing, and

$$\hat{P}_m = P_m + P_p$$

from the IVO timing to the next IVC timing. The superposed pressures $\hat{P}_3$ and $\hat{P}_m$ are the estimated intake manifold pressures of the air model (Fig. 4).

4 CALIBRATION OF AIR MODEL

This chapter sketches how to calibrate behaviors of the air model. The behavior is determined by several parameters, which are divided into two groups. The first group consists of individually identified parameters and the second group is composed of parameters which are calibrated so that the air model fits the real intake system. The first group includes the discharge coefficient C, the cross-sectional area S_1, and so on. The second group comprises the polytropic index n, the cylinder pressure and density at the IVO timing, and the parameters of the intake pulsation. This chapter explains how to calibrate the parameters of the second group.

4-1. POLYTROPIC INDEX

The polytropic index n corresponds to friction losses and thermal exchanges along the flow. The polytropic index can be identified from a differential value of the intake manifold pressure.

Physically, the differential value of the intake manifold pressure is monotonically increasing with respect to the polytropic index. Using the monotonicity, the index is adjusted so that the differential value of the intake manifold pressure of the air model is equal to that of the real engine. The index can be usually represented by a multivariable function of the opening area of the throttle valve and the temperature of the intake manifold.

4-2. PRESSURE AND DENSITY AT IVO

The cylinder pressure and density just before the IVO timing compensates the valve overlap and the exhaust pulsation. Their adjustments are based on the following monotonicity.

- The average of the intake manifold pressure through the intake stroke is monotonically increasing with respect to the cylinder pressure just before the IVO timing.
- The amount of decrease in the intake manifold pressure through the intake stroke is monotonically decreasing with respect to the cylinder density just before the IVO timing.

The parameters depend strongly on the mass of the intake air in the last cycle, the elapsed time from the last EVC timing, and so on.

Table 1: Summary of Experiment

Engine	499.5[cc]/2-cylinder (249.8[cc] per cylinder), 360[deg] phase shift, -11.4(Closed) ~ 40.0(WOT) [Nm] @4000[rpm]
M.O.I.	0.177[kg m^2](low) ~ 1.242[kg m^2](top) (equivalent M.O.I. about the crank shaft including the mass of the motorcycle)
Temp.	Atom. 20[degC], Oil 85[degC], Coolant 80[degC]

4-3. INTAKE PULSATION

Since the intake pulsation is triggered by the water hammer effect, the initial amplitude and the initial phase angle are functions of the mass flow rate at the last IVC timing. Moreover, the damping time constant and the angular velocity are functions of a temperature of the intake air.

5 EXPERIMENTAL RESULTS

In Table 1, our experimental conditions are summarized. Figures 6 and 7 compare the intake manifold pressures of the air model and the real engine. The thick lines and the thin lines are the estimated intake manifold pressures and the measured intake manifold pressures, respectively. Moreover, the dashed lines represent their throttle valve positions.

Figure 6 plots the intake manifold pressures in a stationary operation where the engine rotational velocity was 4000 [rpm] and the throttle angle was 15 [deg]. Figure 7-top shows transient responses of the pressures when the throttle valve was opened rapidly from 7 to 70 [deg], and Fig. 7-bottom shows those when the throttle valve was closed rapidly from 50 to 7 [deg]. In any of these cases, the air model estimated the intake manifold pressures with a margin of error of plus or minus five percentage points except for the periods of the valve overlaps.

6 CONCLUSION

This paper describes the simplified calculation method for embedded computers to estimate the intake manifold pressure in real time. The method is derived from the thermodynamic equations and statistical models of the intake air dynamics. In the experiments, the estimation errors were less than five percentage points except for the periods of the valve overlaps.

Continued studies are required in order to improve the accuracy during the periods of the valve overlaps. The problem is a trade-off between computational complexity and gained benefits.

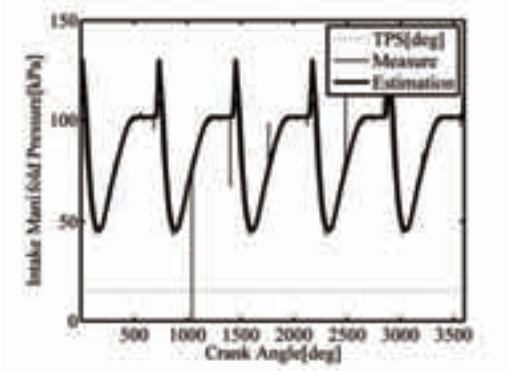

Figure 6: The stationary response at 4000[rpm].

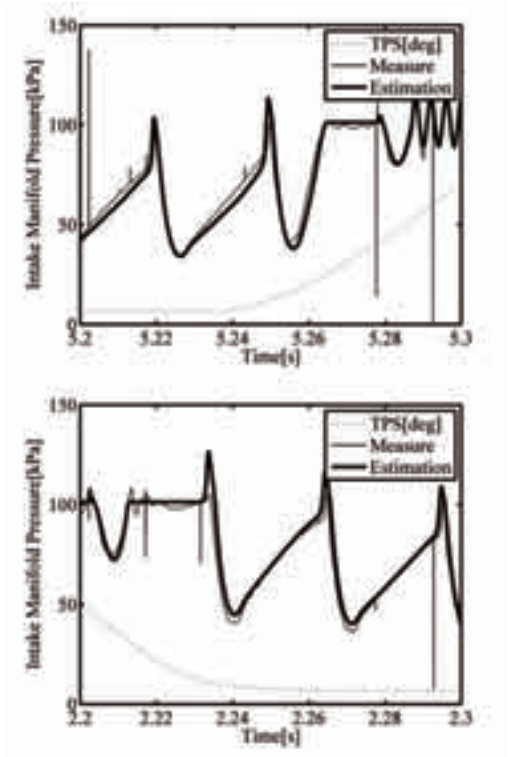

Figure 7: The transient responses around 4000[rpm].

REFERENCES

[1] Toyota Motor Corporation and Toyota Central R&D Labs., Inc., "Instrument for Estimation of Intake Volume in Internal-combustion Engine (in Japanese)," Japanese published unexamined application, 2004-293546 (P2004-293546A), 2004

[2] Siemens Aktiengesellschaft, "Method for determining an air mass flow into cylinders of an internal combustion engine with the aid of a model," United States Patent, 5889205, 1996

[3] Honda Motor Co., Ltd., "Instrument for Control of Fuel Injection in Internal-combustion Engine (in Japanese)," Japanese Patent, No. 3119465 (P3119465), 1993

[4] Yamaha Motor Co., Ltd., "Model-base Control Methodology and Apparatus (in Japanese)," Japanese Patent, P3703117, 1998

[5] Wu, Y.Y., Chen, B.C., and Hsieh, F.C., "Modulization of four-stroke single-cylinder spark-ignition air-cooled engine models," Proc. Inst. Mech. Eng. Part D, Vol. 221, Issue 8, 2007

[6] OPAL-RT TECHNOLOGIES Inc., GT-Power RT, http://www.opal-rt.com/product/gt-power/

[7] Ricardo plc, WAVE-RT, http://www.ricardo.com/What-we-do/Software/Products/WAVE-RT/

[8] Nissan Motor Co., Ltd., "Instrument for Calculation of Residual Gas Density in Engine (in Japanese)," Japanese published unexamined application, 2009-198499 (P2009-198499), 2009

[9] Hitachi Automotive Systems, Ltd., "Estimation Method of Residual Gas Amount in Engine and Control Method of Variable Valve Timing System (in Japanese)," Japanese published unexamined application, 2002-205878 (P2002-205878), 2002

[10] Chiang, C.J, "A physics-based model of a HCCI engine with electric mechanical valves," 2008 IEEE Int. Conf. on Sustainable Energy Tech., 2008

[11] SuperFlow Corp., SF-1020,http://www.superflow.com/

[12] S. Akama, Y. Murayama, and S. Sakoda, "Torque Control of Rear Wheel by Using Inverse Dynamics of Rubber/Aramid Belt Continuous Variable Transmission, "Proc. of SETC 2013, Taiwan, 2013

■著者

赤間 俊一
Shun-ichi Akama
技術本部
研究開発統括部
基盤技術研究部

村山 恭規
Yasunori Murayama
技術本部
研究開発統括部
基盤技術研究部

迫田 茂穂
Shigeho Sakoda
技術本部
研究開発統括部
先進技術研究部